JCTC Journal of Chemical Theory and Computation

Efficient Approach to Reactive Molecular Dynamics with Accurate Forces

Masahiro Higashi and Donald G. Truhlar*

Department of Chemistry and Supercomputing Institute, University of Minnesota, 207 Pleasant Street SE, Minneapolis, Minnesota 55455-0431

Received June 11, 2009

Abstract: Density functional theory is a powerful and efficient method for calculating potential energy surfaces for chemical reactions, but its application to complex systems, such as reactions in enzymes, is often prohibitively expensive, even when high-level theory is applied only to a primary subsystem, such as an active site, and when the remaining system is treated by molecular mechanics. Here we show how the combination of multiconfiguration molecular mechanics with charge response kernels can speed up such calculations by three or more orders of magnitude. The resulting method, called electrostatically embedded multiconfiguration molecular mechanics, is illustrated by calculating the free energy of activation profile for the dehalogenation of 1,2-dichloroethane by haloalkane dehalogenase. This shows how hybrid density functionals or other high-level electronic structure methods can now be used efficiently in simulations that require extensive sampling, such as for calculating free energy profiles along a high-barrier reaction coordinate.

"The accuracy of a simulation is largely determined by two factors: conformation sampling and model accuracy."[1] The Car−Parrinello scheme[2] created a paradigm shift in molecular dynamics simulations by suggesting an efficient way to replace empirical interatomic potential models (molecular mechanics) with density functional direct dynamics, where direct dynamics implies that "instead of using a pre-defined PEF (potential energy function), all required energies and forces for each geometry that is important for evaluating dynamical properties are obtained directly from electronic structure calculations."[3] Now density functional direct dynamics, using either the Car−Parrinello algorithm or later-generation ones, is a standard tool in materials science,[4,5] especially with density functionals that do not involve nonlocal operators because local functionals allow for less expensive plane wave calculations on extended systems. In some cases, density functional theory (DFT) is replaced by another quantum mechanical (QM) method, or QM is applied to an active site subsystem and combined with molecular mechanics (MM) for a much larger secondary subsystem. For many problems, though, such as free energy simulations of enzyme-catalyzed reactions, even combined QM/MM calculations are very expensive because of the required QM system size or the large amount of sampling required, and there is considerable research on how to make the calculations most affordable.[6−15]

The most accurate QM levels for chemistry require inclusion of dynamical correlation and nonlocal Hartree−Fock exchange, as in hybrid density functionals that represent a marriage of Kohn−Sham and Hartree−Fock theories,[16] but Hartree−Fock exchange makes calculations on large or complex systems very expensive. In the present article, we report well-converged free energy simulation of an enzymatic reaction employing a hybrid density function that includes 42.8% Hartree−Fock exchange. This calculation is made efficient by applying the new electrostatically embedded multiconfiguration molecular mechanics (EE-MCMM) algorithm,[17] which is actually a powerful but semiautomatic fitting algorithm that is adapted to be efficient in the combined QM/MM context.

Consider first the MCMM algorithm for a gas-phase reaction[18,19] with N atoms with coordinates $\mathbf{R}_\alpha \equiv (X_\alpha, Y_\alpha, Z_\alpha)$, $\alpha = 1, 2, ..., N$, and let $\mathbf{R}$ denote the set of $\mathbf{R}_\alpha$. MCMM involves approximating the PEF as the lowest eigenvalue V of a 2×2 valence bond configuration interaction matrix:[20]

$$\mathbf{H} \equiv \begin{pmatrix} H_{11} & H_{12} \\ H_{12} & H_{22} \end{pmatrix} \tag{1}$$

H_{11} is set equal to the MM PEF of reactants, and the H_{22} is set equal to the MM PEF of products.[21] At a set of K geometries called electronic structure Shepard points, $\mathbf{R}^{(k)}$, with $k = 1, 2, ..., K$, one uses electronic structure theory to calculate a Taylor expansion of V valid through second order in $\mathbf{Q}^{(k)} \equiv \mathbf{R} - \mathbf{R}^{(k)}$. One then re-expresses this as a second-order Taylor expansion $H_{12}^{(k)}$ of $H_{12}(\mathbf{Q})$.[22] A global approximation to H_{12} is then obtained by joining these expansions (possibly augmented by K^{MM} additional points where $H_{12}^{(k)}$ is assumed to be zero) by Shepard interpolation.[18,19,23]

In combined QM/MM treatments of chemical reactions, the reactive QM subsystem interacts with a (usually much larger) nonreactive subsystem described by MM.[24,25] The interaction of the subsystems is described by stretching, bending, torsion,

* Corresponding author. Telephone: 612-624-7555. Fax: 612-624-9390. E-mail: truhlar@umn.edu.

10.1021/ct900301d CCC: $40.75
Published on Web 10/16/2009

noncovalent (repulsion and dispersion), and electrostatic terms. The electrostatic terms are the only ones that affect the QM wave function, and they correspond to including the partial atomic charges of the MM subsystem in the Hamiltonian of the electronic orbitals of the QM subsystem. As in the method of charge response kernels,[26−28] we replace these QM orbital−MM partial charge interactions by QM partial charge−MM partial charge interactions. Then the electrostatic terms depend on the MM system only through the N values Φ_α of the electrostatic potential of the MM subsystem at the nuclei of the QM subsystem. Thus, the QM energy depends on $4N$ variables: X_α, Y_α, Z_α, Φ_α, $\alpha = 1, 2, ..., N$. By using $4N$-dimensional Taylor series (rather than the $3N$-dimensional ones used for gas-phase calculations) in the Shepard interpolation, the MCMM method can treat the electrostatically embedded (EE) QM subsystem of the combined QM/MM calculation very efficiently; this is called EE-MCMM.[17] The new kinds of derivatives that appear in the Taylor series are $\partial V/\partial\Phi_\alpha$, which is a partial charge Q_α on QM atom α, and $\partial^2 V/\partial\Phi_\alpha\partial\Phi_\beta$ and $\partial^2 V/\partial\Phi_\alpha\partial\mathbf{R}_\alpha$, which are charge response kernels that, respectively, describe the QM charge fluctuations due to the MM electrostatic potential and the displacements of the QM atoms. The truncation of the Taylor series in $\phi_\alpha = \Phi_\alpha - \Phi_\alpha^{(k)}$ at second order is adequate because the linear response relation between Q_α and Φ_α generally holds quite well even when ϕ_α is large,[29] and because the trust regions around each $\mathbf{R}^{(k)}$, $\mathbf{\Phi}^{(k)}$ point are merged by Shepard interpolation.

As explained in previous papers,[18,30,31] MCMM[18] is based on a combination of several elements: (i) semiempirical valence bond theory for the potential energy surface V of a chemical reaction,[32] (ii) the combination of semiempirical valence bond theory with MM for spectator degrees of freedom,[31,33] (iii) the empirical valence bond method in which MM force fields are used for the diagonal elements of a valence bond Hamiltonian matrix, and their parameters or parameters in off-diagonal elements (H_{12} in the case of a two-configuration treatment, as used here) can be adjusted to produce either potential energy surfaces or features that agree with electronic structure calculations or features inferred from experiments,[21,34] (iv) the reversion of a Taylor series for V at a particular geometry to provide a Taylor series for H_{12},[22] (v) the multidimensional Shepard interpolation method,[23] and (vi) the efficient and orientation-independent representation of low-order expansions of potential energy surfaces in internal coordinates.[35] MCMM combines these elements in a new way. For example, whereas the Shepard interpolation was originally applied to interpolate V,[23] it is used in MCMM to interpolate H_{12}, which is a key difference because H_{12} is generally more slowly varying and less rugged. MCMM also uses a new weighting function for the Shepard interpolation. EE-MCMM[17] extends MCMM to electronically embedded QM/MM calculations[24,25] by combining MCMM with charge response kernels[26−29] for electrostatic embedding. MCMM is designed to provide a particularly efficient method for fitting global potential energy surfaces of complex systems, and EE-MCMM extends the approach to electronically embedded QM subsystems in combined QM/MM calculations.

We emphasize that, although our method involves MM, its goal is to fit a high-level potential energy surface for a specific multidimensional reaction conveniently and efficiently, not to generate a semiempirical approximation to a surface. Similarly, although the method uses charge response kernels, it is not an alternative to semiempirical fluctuating charge or electronegativity equalization models, but rather it uses these kernels to efficiently represent the response[26−29] calculated for a particular system by a high-level method. If the method is continued to convergence, then the results become independent of the MM force field employed and approach the results that would be obtained with the high-level fitted. However, it is not necessary to converge the calculations to that limit, and we accept a dependence on the assumed MM force field in the reactant and product regions if MM is reasonably accurate there, and we accept an MM dependence in the regions of the surface that are less important for the particular dynamical event under consideration, just as combined QM/MM calculations accept MM for the degrees of freedom of the system that are less strongly coupled to the reaction.

Here we demonstrate the applicability of EE-MCMM to enzyme kinetics by applying it to the reaction $RCH_2C(O)O^- + CH_2ClCH_2Cl \rightarrow RCH_2C(O)OCH_2CH_2Cl + Cl^-$, where R is haloalkane dehalogenase, and the carboxylate nucleophile participating in the reaction is the side chain of Asp124.[36] Because our objective in this letter is to provide a methodological demonstration of capability and reduction to practice, we do not review work whose objective is to understand the particular enzyme reaction used for the example.

Results

Our simulation has 15 QM atoms (substrate plus $CH_2C(O)O^-$ of Asp124) and 5 812 MM atoms (the rest of the protein and water), and we used the hybrid density functional MPW1K,[37] where the fraction of Hartree−Fock exchange was optimized[37] to reproduce barrier heights and reaction energies. As a result, MPW1K includes 42.8% Hartree−Fock exchange, and the error is much smaller than the errors of local density functionals.[38]

The reaction coordinate is defined in terms of the breaking C−Cl bond distance r_1 and the forming C−Cl bond distance r_2 by

$$z = r_1 - r_2 \tag{2}$$

First, we performed constrained optimizations with $z = -0.9$, $+0.2$, and $+1.8$ Å. This yielded three sets ($k = 1, 2, 3$) of $\mathbf{R}^{(k)}$, $\mathbf{\Phi}^{(k)}$ that were used for a preliminary EE-MCMM fit. A minimum-energy path for this fit differed from a full MPW1K/MM calculation by the greatest amount at $z = 0.9$ Å, so that point was chosen as the fourth Shepard point. Four more Shepard points were then added at locations where preliminary MCMM fits differed from full calculations. The final simulations have $K = 8$ and $K^{MM} = 0$.

Figure 1 shows three snapshots from the simulation. These pictures show that two tryptophans make hydrogen bonds with the substrate at the transition state.

We carried out umbrella sampling by the weighted histogram analysis method[39] (WHAM) with 33 equally spaced windows centered at values z_0 of the reaction coordinate from -1.2 to $+2.0$ Å. The resulting potential of mean force (PMF) is shown in Figure 2. The PMF is very smooth and physically reasonable. The barrier in the PMF is 15.3 kcal/mol. Correcting for the vibrational free energy along the reaction coordinate at the reactant[40] lowers this to 14.8 kcal/mol. Since z is nearly linear

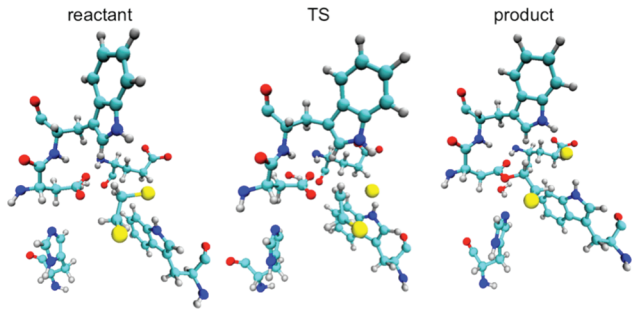

Figure 1. Hydrogen bonding in the active site. Snapshots of the QM subsystem plus key nearby MM atoms at the reactant, the transition state, and the product configurations.

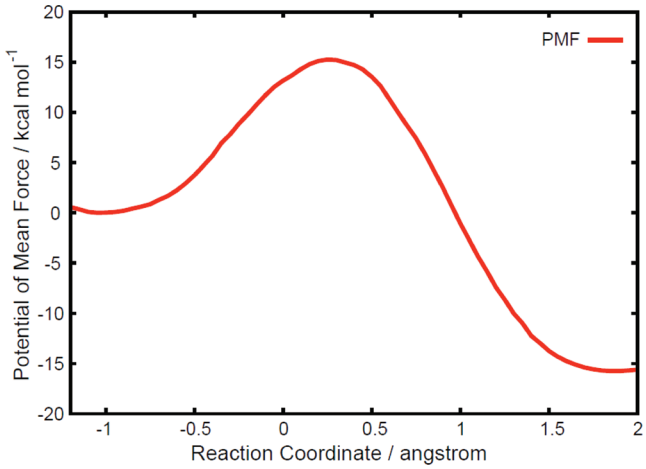

Figure 2. Free energy profile. Free energy as a function of reaction coordinate *z*.

Table 1. Errors (kcal/mol) during MD Simulations

z_0	mean signed error	mean unsigned error
−0.8	−0.3	1.1
−0.4	−0.3	0.6
0.0	−0.5	0.8
+0.4	−0.2	0.5
+0.8	0.5	0.8
+1.2	0.3	0.9
+1.6	0.7	0.9
all[a]	0.1	0.9

[a] 3 300 configurations from all windows with $-1.2 \le z_0 \le 2.0$ Å.

in Cartesian coordinates at the transition state, this may be considered to be a good approximation to the free energy of activation.[40] For comparison, the experimental value is 15.3 kcal/mol (obtained from the experimental rate constant[41] using transition-state theory).

During the umbrella sampling run, we saved a configuration every 0.5 ps during the data collection phase for each window, for a total of 3 300 configurations in the entire umbrella sampling calculations. We then compared the EE-MCMM/MM energies at these points to full QM/MM calculations; the error statistics are given in Table 1. This table shows that the mean signed and unsigned errors in the PEF are reasonably small all along the reaction path.

Discussion

Combined QM/MM methods are a powerful means for studying chemical reactions in solution, enzymes, and solids. Two central difficulties are using a reliable level for the QM subsystem and sampling configurations of the entire system adequately. It is difficult to carry out direct high-level ab initio or density functional calculations because both types of calculations require a high computational cost. Here we have shown that the EE-MCMM method has great promise for describing QM/MM potential energy surfaces for free energy calculations in enzyme kinetics with electronically embedded QM subsystems with reliable accuracy and low computational cost.

Table 2 compares the computational cost for the calculations presented here to the estimated computer time for straight direct dynamics without EE-MCMM. The EE-MCMM algorithm speeds up the calculation for a total simulation time of 3.3 ns by an estimated factor of 950. The ratio would become even more favorable if longer sampling times were required because in EE-MCMM the extra cost above using analytic potential energy surfaces is all up front. Therefore, EE-MCMM makes QM/MM with hybrid density functionals affordable for large and complex systems requiring extensive sampling, such as high-barrier enzymatic reactions.

Although the errors in Table 1 are small, using more than eight Hessians could reduce them further. We chose instead to show how well we can do with a very small number of Hessians. In most cases, there is a law of diminishing returns where the precision of the fit is reduced below the level of intrinsic accuracy of the underlying electronic structure method. A recent study[38] showed a mean unsigned error of 1.6 kcal/mol for MPW1K with a comparable basis to that used here, where the error was assessed with a representative database of S_N2 barrier heights (as compared to 8.7 kcal/mol for the popular[11,15] local functional BLYP with the largest basis set tested — larger than the one used here), so the mean errors in Table 1 are already less than the errors due to the inexactness of the underlying density functional. The MM force fields were not optimized for the present work, and the success of the method with standard force fields is one of the attractive features of the method. Nevertheless, although the errors are already acceptably small, we expect that they could be further reduced, if desired, by using optimized or specific reaction parameters in the MM.[42]

A potential speedup is to use analytic Hessians, which are available in many computer codes. Here we used numerical Hessians. We estimate that using analytic Hessians for $\partial^2 V/\partial \mathbf{R}_\alpha \partial \mathbf{R}_\beta$ would have decreased the cost for the Hessian step from 96 to 55 CPU hours. Analytic Hessians for $\partial^2 V/\partial \Phi_\alpha \partial \Phi_\beta$ and $\partial^2 V/\partial \Phi_\alpha \partial \mathbf{R}_\alpha$ are also available,[27] and using these would further reduce the computational time. Further efficiency could be also achieved by using partial electronic structure Hessians[43] or by using the new non-Hermitian formulation of MCMM.[44]

Methods

As the starting geometry, we used the X-ray crystal structure of the enzyme−substrate complex (Protein Data Bank code 2DHC).[36] The basis set for the quantal calculations was 6-31(+)G(d,p).[16] The MM force fields were modified MM3 (where the modifications were described previously[16]) for the substrate, AMBER ff03[1] for the protein, and TIP3P[45] for water. Partial charges were obtained by Charge Model 4 (CM4)[16,46] for the QM region and by RESP[1,47] for the MM subsystem.

Table 2. Computational Costs[a]

task	CPU hours
QM/MM geometry optimizations for a reaction path to guide Shepard point placement[b]	68
eight four-dimensional (X_α, Y_α, Z_α, Φ_α) Hessians at Shepard points[b]	96
EE-MCMM/MM MD simulations (31 windows, each with 50 ps of equilibration and 50 ps of data collection[c]	528
total	692
direct QM/MM simulations (estimated)	$\sim 6.6 \times 10^5$

[a] CPU hours = CPUs × hours on an SGI Altix XE 1300 Linux cluster with 2.66 GHz Intel Xeon processors. [b] Four CPUs, GAMESSPLUS. [c] Two CPUs, AMBER with MC-TINKER. One processor calculates H_{11}, and the other calculates H_{22}.

The interface between the QM and MM subsystems was treated by the link atom method[48] with the balanced[49,50] RC[51] scheme.

The umbrella sampling was carried out at $T = 300$ K to calculate the PMF. The equations of motion were integrated by the velocity Verlet method with a time step of 0.5 fs. For each umbrella sampling window, we began with a 50 ps MD trajectory calculation for equilibration, followed by 50 ps calculation for statistical sampling. The negative contribution of the reaction-coordinate motion of the reactant to the free energy of activation[40,52] was included by subtracting the vibrational free energy along the reaction coordinate at the reactant:

$$G_{\mathrm{R},z} = -k_{\mathrm{B}}T \ln \frac{k_{\mathrm{B}}T}{\hbar\omega_{\mathrm{R},z}} \tag{3}$$

from the PMF where k_{B}, T, and $\hbar$ are the Boltzmann constant, temperature, and Planck's constant divided by 2π. The effective vibrational frequency $\omega_{\mathrm{R},z}$ of the reaction coordinate at the reactant was calculated from a force constant obtained from the PMF around the reactant and an averaged reduced mass calculated in the reactant window using eq 38 in ref 40.

In applying MCMM or EE-MCMM, the quadratic Taylor series are expressed in internal coordinates for the interpolation step. For a shallow potential along a torsion coordinate, Θ_m (where m is a label distinguishing the various torsions), the second-order truncation is sometimes problematic. Therefore we replace $\theta_m = \Theta_m - \Theta_m^{(k)}$ by $\sin(n_{\Theta_m}(\Theta_m - \Theta_m^{(k)}))/n_{\Theta_m}$, where n_{Θ_m} is 1 for an X−C−O−Y torsion and 3 for an X−C−C−Y torsion. Furthermore, we set some of the quadratic coefficients involving torsions equal to zero.

The electronic structure calculations were carried out by GAMESSPLUS[53,54] in which we implemented the QM/MM optimization program. The dynamics calculations were carried out by a locally modified version of AMBER[55] with MC-TINKER.[56,57] The WHAM calculations were carried out with a program written by Grossfield.[58]

Acknowledgment. This work was supported in part by the National Science Foundation (grant CHE07-04974, supporting quantum mechanical methods for complex chemical systems) and by the Office of Naval Research (award N00014-05-0538, supporting integrated software tools for dynamics).

References

(1) Duan, Y.; Wu, C.; Chowdhury, S.; Lee, M. C.; Xiong, G.; Zhang, W.; Yang, R.; Cieplak, P.; Luo, R.; Lee, T.; Caldwell, J.; Wang, J.; Kollman, P. *J. Comput. Chem.* **2003**, *24*, 1999.

(2) Car, R.; Parrinello, M. *Phys. Rev. Lett.* **1985**, *55*, 2471.

(3) Liu, Y.-P.; Lu, D.-H.; Gonzalez-Lafont, A.; Truhlar, D. G.; Garrett, B. C. *J. Am. Chem. Soc.* **1993**, *115*, 7806.

(4) Tse, J. S. *Annu. Rev. Phys. Chem.* **2002**, *53*, 249.

(5) Huang, P.; Carter, E. A. *Annu. Rev. Phys. Chem.* **2008**, *59*, 261.

(6) Gao, J.; Truhlar, D. G. *Annu. Rev. Phys. Chem.* **2002**, *53*, 467.

(7) Claeyssens, F.; Harvey, J. N.; Manby, F. R.; Mata, R. A.; Mulholland, A. J.; Ranaghan, K. E.; Schütz, M.; Thiel, S.; Thiel, W.; Werner, H.-J. *Angew. Chem., Int. Ed.* **2006**, *45*, 6856.

(8) Senn, M.; Thiel, W. *Curr. Opinion Chem. Biol.* **2007**, *11*, 182.

(9) Lin, H.; Truhlar, D. G. *Theor. Chem. Acc.* **2007**, *117*, 185.

(10) Hu, H.; Yang, W. *Annu. Rev. Phys. Chem.* **2008**, *59*, 573.

(11) DeVivo, M.; Dal Peraro, M.; Klein, M. L. *J. Am. Chem. Soc.* **2008**, *130*, 10955.

(12) Wu, X.; Car, R.; Selloni, A. *Phys. Rev. B: Solid State* **2008**, *79*, 085102.

(13) Hu, P.; Wang, S.; Zhang, Y. *J. Am. Chem. Soc.* **2008**, *130*, 16721.

(14) Neese, F.; Wennohs, F.; Hansen, A.; Becker, U. *Chem. Phys.* **2009**, *356*, 98.

(15) Masson, F.; Laino, T.; Rothlisberger, U.; Hutter, J. *ChemPhysChem* **2009**, *10*, 400.

(16) Kohn, W.; Becke, A. D.; Parr, R. G. *J. Phys. Chem.* **1996**, *106*, 12974.

(17) Higashi, M.; Truhlar, D. G. *J. Chem. Theory Comput.* **2008**, *4*, 790.

(18) Kim, Y.; Corchado, J. C.; Villa, J.; Xing, J.; Truhlar, D. G. *J. Chem. Phys.* **2000**, *112*, 2718.

(19) Tishchenko, O.; Truhlar, D. G. *J. Chem. Phys.* **2009**, *130*, 024105.

(20) Eyring, H.; Walter, J.; Kimball, G. *Quantum Chemistry*; Wiley: New York, 1944.

(21) Warshel, A.; Weiss, R. M. *J. Am. Chem. Soc.* **1980**, *102*, 6218.

(22) Chang, Y.-T.; Miller, W. H. *J. Phys. Chem.* **1990**, *94*, 5884.

(23) (a) Ischtwan, J.; Collins, M. A. *J. Chem. Phys.* **1994**, *100*, 8080. (b) Nguyen, K. A.; Rossi, I.; Truhlar, D. G. *J. Chem. Phys.* **1995**, *102*, 5522. (c) Thompson, K. C.; Jordan, M. J. T.; Collins, M. A. *J. Chem. Phys.* **1998**, *108*, 8302.

(24) Gao, J. *Rev. Comp. Chem.* **1995**, *7*, 119.

(25) For recent reviews, see refs 9 and 10 and (a) Friesner, R. A.; Guallar, V. *Annu. Rev. Phys. Chem.* **2005**, *56*, 389. (b) Senn, H.-M.; Thiel, W. *Top. Curr. Chem.* **2007**, *268*, 173. (c) Lodola, A.; Woods, C. J.; Mulholland, A. J. *Annu. Rep. Comp. Chem.* **2008**, *4*, 155.

(26) Morita, A.; Kato, S. *J. Am. Chem. Soc.* **1997**, *119*, 4021.

(27) Ishida, T.; Morita, A. *J. Chem. Phys.* **2006**, *125*, 074112.

(28) Lu, Z.; Yang, W. *J. Chem. Phys.* **2004**, *121*, 89.

(29) Morita, A.; Kato, S. *J. Chem. Phys.* **1998**, *108*, 6809.

(30) Albu, T. V.; Corchado, J. C.; Truhlar, D. G. *J. Phys. Chem. A* **2001**, *105*, 8465.

(31) Albu, T. V.; Corchado, J. C.; Truhlar, D. G. *Chem. Rev.* **2007**, *107*, 5101.

(32) For reviews, see: (a) Eyring, H. *Trans. Faraday Soc.* **1938**, *34*, 3. (b) Parr, C. A.; Truhlar, D. G. *J. Phys. Chem.* **1971**, *75*, 1844.

(33) Raff, L. M. *J. Chem. Phys.* **1974**, *60*, 2222.

(34) (a) Hwang, J.-K.; King, G.; Creighton, S.; Warshel, A. *J. Am. Chem. Soc.* **1988**, *110*, 5297. (b) Bentzien, J.; Muller, R. P.; Florián, J.; Warshel, A. *J. Phys. Chem. B* **1998**, *102*, 2293.

(35) (a) Fogarasi; Pulay, P. In *Vibrational Spectra and Structure*; Durig, J. R., Ed.; Elsevier: Amsterdam, 1985; Vol. 14, p. 125. (b) Jackels, C. F.; Gu, Z.; Truhlar, D. G. *J. Chem. Phys.* **1995**, *102*, 3188. (c) Chuang, Y.-Y.; Truhlar, D. G. *J. Phys. Chem. A* **1998**, *102*, 242.

(36) Verschueren, K. H.; Seljée, F.; Rozeboom, H. J.; Kalk, K. H.; Dijkstra, B. W. *Nature* **1993**, *363*, 693.

(37) Lynch, B. J.; Fast, P. L.; Harris, M.; Truhlar, D. G. *J. Phys. Chem. A* **2000**, *104*, 4811.

(38) Zheng, J.; Truhlar, D. G. *J. Chem. Theory Comput.* **2009**, *5*, 808.

(39) Kumar, S.; Rosenberg, J. M.; Bouzida, D.; Swendsen, R. H.; Kollman, P. A. *J. Comput. Chem.* **2004**, *13*, 1011.

(40) Schenter, G. K.; Garrett, B. C.; Truhlar, D. G. *J. Chem. Phys.* **2003**, *119*, 5828.

(41) Schanstra, J. P.; Kingma, J.; Janssen, D. B. *J. Biol. Chem.* **1996**, *271*, 14747.

(42) Tishchenko, O.; Truhlar, D. G. *J. Phys. Chem. A* **2006**, *110*, 13530.

(43) Lin, H.; Pu, J.; Albu, T. V.; Truhlar, D. G. *J. Phys. Chem. A* **2004**, *108*, 4112.

(44) Tishchenko, O.; Truhlar, D. G. *J. Chem. Theory Comput.* **2009**, *5*, 1454.

(45) Jorgensen, W. L.; Chandrasekhar, J.; Madura, J. D.; Impey, R. W.; Klein, M. L. *J. Chem. Phys.* **1983**, *79*, 926.

(46) Kelly, C. P.; Cramer, C. J.; Truhlar, D. G. *J. Chem. Theory Comput.* **2005**, *1*, 1133.

(47) Bayly, C. I.; Cieplak, P.; Cornell, W. D.; Kollman, P. A. *J. Phys. Chem.* **1993**, *97*, 10269.

(48) Singh, U. C.; Kollman, P. A. *J. Comput. Chem.* **1986**, *7*, 718.

(49) Walker, R. C.; Crowley, M. F.; Case, D. A. *J. Comput. Chem.* **2008**, *29*, 1013.

(50) Wang, B.; Truhlar, D. G. J. Chem. Theory Comput., in press.

(51) Lin, H.; Truhlar, D. G. *J. Phys. Chem. A* **2005**, *109*, 3991–2005.

(52) Alhambra, C.; Corchado, J.; Sánchez, M. L.; Garcia-Viloca, M.; Gao, J.; Truhlar, D. G. *J. Phys. Chem. B* **2001**, *105*, 11326.

(53) Higashi, M.; Marenich, A. V.; Olson, R. M.; Chamberlin, A. C.; Pu, J.; Kelly, C. P.; Thompson, J. D.; Xidos, J. D.; Li, J.; Zhu, T.; Hawkins, G. D.; Chuang, Y.-Y.; Fast, P. L.; Lynch, B. J.; Liotard, D. A.; Rinaldi, D.; Gao, J.; Cramer, C. J.; Truhlar, D. G. *GAMESSPLUS, version 2008−2*; University of Minnesota: Minneapolis, MN, 2008.

(54) Schmidt, M. W.; Baldridge, K. K.; Boatz, J. A.; Elbert, S. T.; Gordon, M. S.; Jensen, J. H.; Koseki, S; Matsunaga, N.; Nguyen, K. A.; Su, S. J.; Windus, T. L.; Dupuis, M.; Montgomery, J. A. *J. Comput. Chem.* **1993**, *14*, 1347.

(55) Case, D. A.; Darden, T. A.; Cheatham, III; T. E.; Simmerling, C. L.; Wang, J.; Duke, R. E.; Luo, R.; Crowley, M.; Walker, R. C.; Zhang, W.; Merz, K. M.; Wang, B.; Hayik, S.; Roitberg, A.; Seabra, G.; Kolossváry, Wong, K. F.; Paesani, F.; Vanicek, J, Wu, X.; Brozell, S. R.; Steinbrecher, T.; Gohlke, H.; Yang, L.; Tan, C.; Mongan, J.; Hornak, V.; Cui, G.; Mathews, D. H.; Seetin, M. G.; Sagui, S.; Babin; V. Kollman, P. A. *AMBER, version 10*; University of California: San Francisco, CA, 2008.

(56) Tishchenko, O.; Higashi, M.; Albu, T. V.; Corchado, J. C.; Kim, Y.; Villà, J.; Xing, J.; Lin, H.; Truhlar, D. G. *MC-TINKER, version 2008−2*; University of Minnesota: Minneapolis, MN, 2008.

(57) Ponder, J. W. *TINKER, version 3.5*; Washington University: St. Louis, MO, 1997.

(58) Grossfield, A. *WHAM, version 2.0.2*; University of Rochester: Rochester, NY, 2008.

CT900301D